第 10卷 第 4期
2006年 7月

遥 感 学 报
JOURNAL OF REMOTE SENSING

Vol. 10, No. 4
July, 2006

文章编号：1007-4619(2006)04-0578-08

A Comparative Study of Image Fusion for Land Cover Classification

WU Meng-che[1], CHEN Kun-shan[1,2]

(1. Institute of Space Science; 2. Center for Space and Remote Sensing Research, Central University, Taiwan, China)

Abstract: There are two main topics to be discuss in this paper: pixel-level image fusion based on Principle Component Analysis (PCA), and feature-level image fusion based on Dempster-Shafer evidence theory. In pixel-level case, the SAR image at HV polarization is relatively sensitive to the vegetation canopy. We combined the HV polarization information from SAR and spectral characteristic from SPOT images in an effort to enhance land cover classification. Before the fusion process, wavelet transform was first applied to denoise the SAR image which suffers from speckle contamination due to coherent process. PCA method is then used to fuse the SPOT and SAR images. In doing so, the PC-1 component is replaced by SAR image (approximation image after wavelet transform) and then the inverse transform is followed. At last, the maximum likelihood classifier was used for both SPOT-XS images and fusion images. In feature-level case, fully polarization information from SAR is used to combine with spectral characteristic from SPOT images, mainly to enhance land cover classification. We first denoise the SAR image by Lee filter. Next, the maximum likelihood classifier based on different distribution was used for SAR and SPOT images (Based on Wishart distribution and multivariate Gaussian distribution respectively), to extract the conditional probability of each pixel for each class. Dempster-Shafer evidence theory is then applied, to combine the classified results of SAR and SPOT data. Experimental results show that the classification accuracy is dramatically improved by making use of the proposed methods. Data fusion can take advantage of the use of complementary information to obtain a better overall accuracy than using single data source only.

Key words: pixel-level image fusion; feature-level image fusion; wishart distribution

Document code: TP751.1 **CLC number:** A

影像融合技术应用于地表分类之探讨

吴孟哲[1]，陈锟山[1,2]

（1. 太空科学研究所；2. 太空及遥测研究中心，中央大学，中国 台湾）

摘 要： 本论文尝试讨论两个主题：主题一为利用主成分分析 PCA 方法应用于像元阶层资料融合技术的研究。主题二为应用 Dempster-Shafer evidence theory方法于特征阶层数据融合技术的研究。在第一个主题中，由于合成孔径雷达的数据具有全偏极特性，在此选取了对植被较为敏感的 HV 极化合成孔径雷达数据，与具有光谱特性的光学 SPOT数据做数据融合处理以利接下来的地物分类。首先，本研究利用小波转换技术来滤除合成孔径雷达斑驳噪声，在接下来融合步骤中，主成分分析出来的第一部分（PC1）是用做完滤除噪声后的合成孔径雷达取代，在数据融合后，进行地物分类是采用最大似然法来分类融合影像。在第二个主题中，利用全偏极雷达数据的极化特性结合 SPOT数据的光谱特性，其主要目的是为了增加分类的精确度。首先使用李式滤波器滤除全偏极雷达数据噪声，接下来同样是使用采用最大似然法来分类融合影像，（不同的在于全偏极雷达影像使用 Wishart几率分布，在光学

Received data: 2005-08-15

影像采用 multivariate Gaussian几率分布)将每个类别中每个像元属于某个类别的几率值计算出来，再利用 Dempster Shafer evidence theory来结合这些类别的机率值。最后产生出一张新的分类影像。实验的结果显示分类的精确度比较于未融合的资料都有明显提升的效果，也证明了此两个数据融合方法对于不同数据特性的融合都是很成功的。

关键词：　像元等级影像融合；特征等级影像融合；Wishart分布

1 INTRODUCTION

Image fusion is a process dealing with data and information from multiple sources to achieve refined / improve information for decision making[1]. A general definition of image fusion is given as "Image fusion is the combination of two or more different images to form a new image by using a certain algorithm"[2]. Image fusion is performed at three different processing levels according to the stage at which the fusion takes place (Fig 1).

1. Pixel-level
2. Feature-level
3. Decision-level

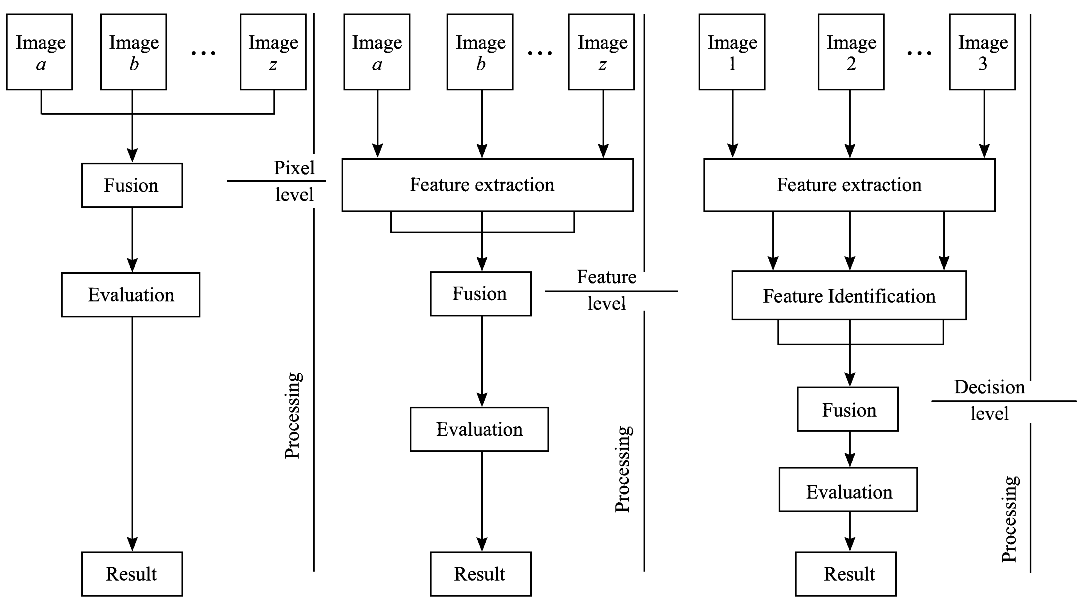

Fig 1　Processing levels of image fusion

Image fusion is a tool to combine multisource imagery using advanced image processing techniques. It aims at the integration of disparate and complementary data to enhance the information apparent in the images as well as to increase the reliability of interpretation. This leads to more accurate data[3] and increased utility[4]. There are two main topics in this study, pixel-level image fusion and feature-level image fusion. In pixel-level case, before the fusion process, wavelet transform was first applied to denoise the SAR image which suffers from speckle contamination due to coherent process. PCA method is then used to fuse the SPOT and SAR images. In so doing, the PC-1 component is replaced by SAR image (approximation image, after wavelet transform) and then the inverse transform is followed. The maximum likelihood classifier was used for both SPOT-XS images and fusion images at the last of the fusion process. For the feature-level case, Lee filter was first applied to denoise the SAR image which suffers from speckle contamination due to coherent process. The maximum likelihood classifier was used for both SAR and SPOT images, to extract the conditional probability of each pixel for each class. Dempster-Shafer evidence theory[5] is applied next, to combine the classified results of SAR and SPOT data.

2 METHODOLOGY

2.1 Pixel-level Image Fusion

As the previous section mentioned about pixel-level image fusion, the different images to be fused can come from different sensors of the same basic type or they may come from different types of sensors. The sensors used for image fusion need to be accurately co-aligned so that their images will be in spatial registration. In this study, we combined the polarization information from SAR and spectral characteristic from SPOT images in an effort to enhance land cover classification. Before the fusion process, wavelet transform was first applied to denoise the SAR image which suffers from speckle contamination due to coherent process. PCA method is then used to fuse the SPOT and SAR images. In so doing, the first component (PC-1) from the PCA is replaced by SAR image (approximation image, after wavelet transform) and then the inverse transform is followed. The maximum likelihood classifier was used for both SPOT-XS images and fused images. The overall accuracy and kappa coefficient were evaluated at the last. Fig. 2 shows the working flowchart of pixel-level image fusion.

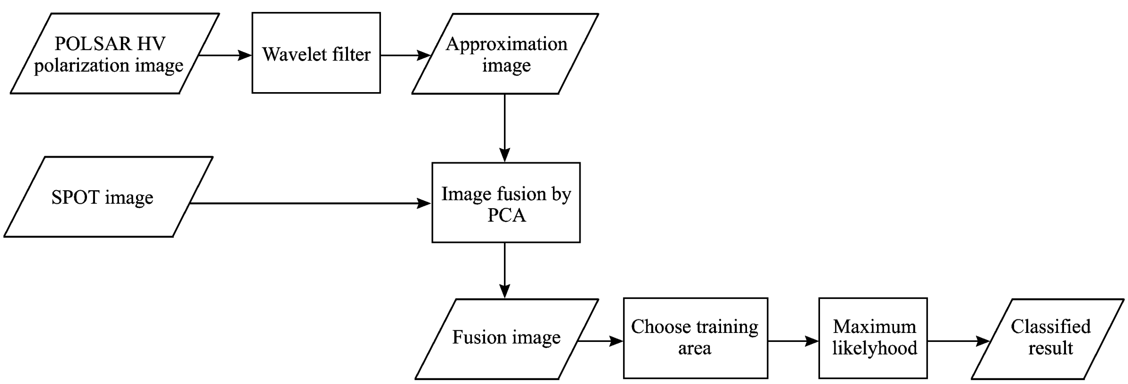

Fig. 2 Working flowchart of pixel-level image fusion

2.2 Feature-level Image Fusion

As shown Fig. 1, images acquired over the same site by different sensors are generally partially redundant, as they represent the same scene, and partially complementary, since the sensors have different characteristics and physical interaction mechanisms are different. For many applications of image classification problems, the information provided by a single sensor is incomplete resulting in misclassification. Fusion with redundant data can help reduce imprecision, and fusion with complementary data can provide a more complete description. In both cases, classification results should be better. For the feature-level case, Lee filter was first applied to denoise the SAR image which suffers from speckle contamination due to coherent process. The maximum likelihood classifier was used for both SAR and SPOT images, to extract the conditional probability of each pixel for each class. Dempster-Shafer evidence theory[5] is applied next, to combine the classified results of SAR and SPOT data. Fig. 3 shows the working flowchart of feature-level image fusion.

3 EXPERIMENTAL TEST RESULTS

3.1 Test Data Sets Description

The fully polarimetric SAR (POLSAR) data set was acquired during the 2000 Pacrim-II campaign over plantation Au-Ku in western of Taiwan. P-L-C-band polarimetric SAR data were collected and processed. Ground truth work was conducted when the data was taken. From the site survey, a total of seven classes to be classified were determined: Sea, Sugarcane type A, Sugarcane type B, Bare-soil, Grass, Building and Rice. The POLSAR image (L-band) at HV polarization is relatively sensitive to the vegetation canopy. The reason why we do not use C-band is that it has shorter

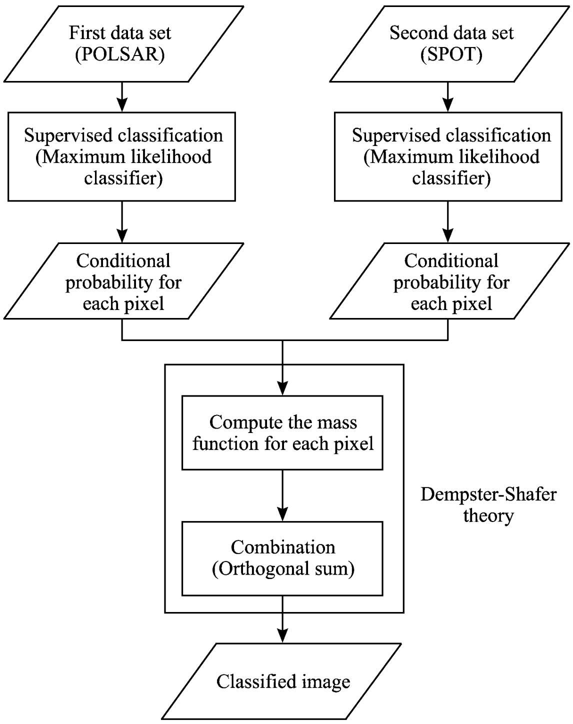

Fig 3 Working flow chart of feature level image fusion

wavelength and so it could not measure the structure of vegetation. Therefore, HV polarization will be used as the experimental test area in pixel-level image fusion. POLSAR L-band data is used for feature level image fusion. The optical image which acquired by SPOT 4, was taken the same test area as POLSAR test image (Fig 4).

3.2 Classification Results of Pixel-level Image Fusion

After the fusion process, maximum likelihood classifier has been applied for both SPOT and fusion data. Fig 5 shows the fusion image. Fig 6 shows the classified results for both fusion image and SPOT image. Table 1 and table 2 show the error matrix for both classified results. The overall accuracy and kappa coefficient for SPOT classified result are 79.05% and 71.62% respectively. For fused image classified results are 97.51% and 96.57% respectively.

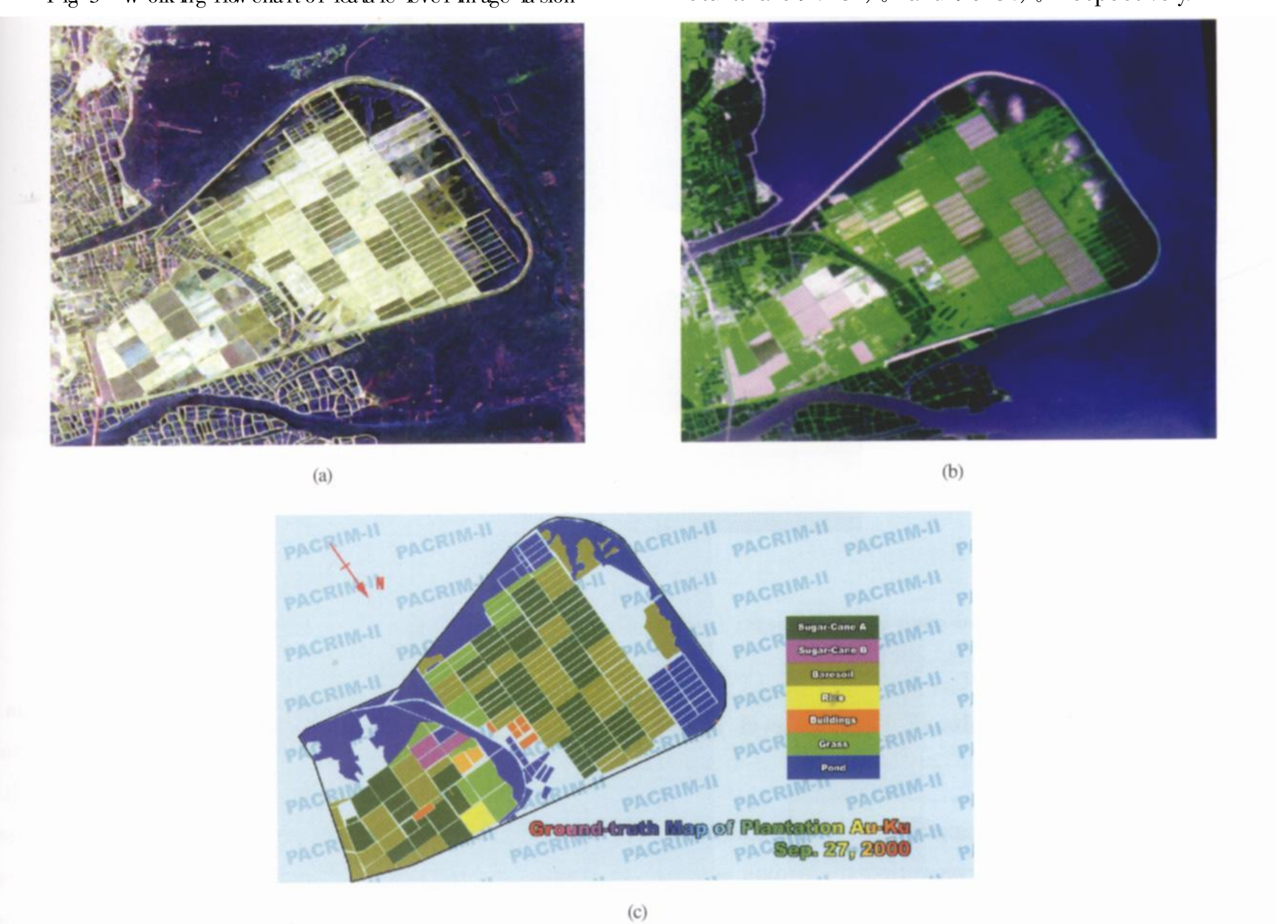

Fig. 4 (a) POLSAR data: R:HH, G:HV, B:VV; (b) SPOT data: R:Band 2, G:Band 3, B:Band 1; (c) Ground truth data

Fig.5 Fused image

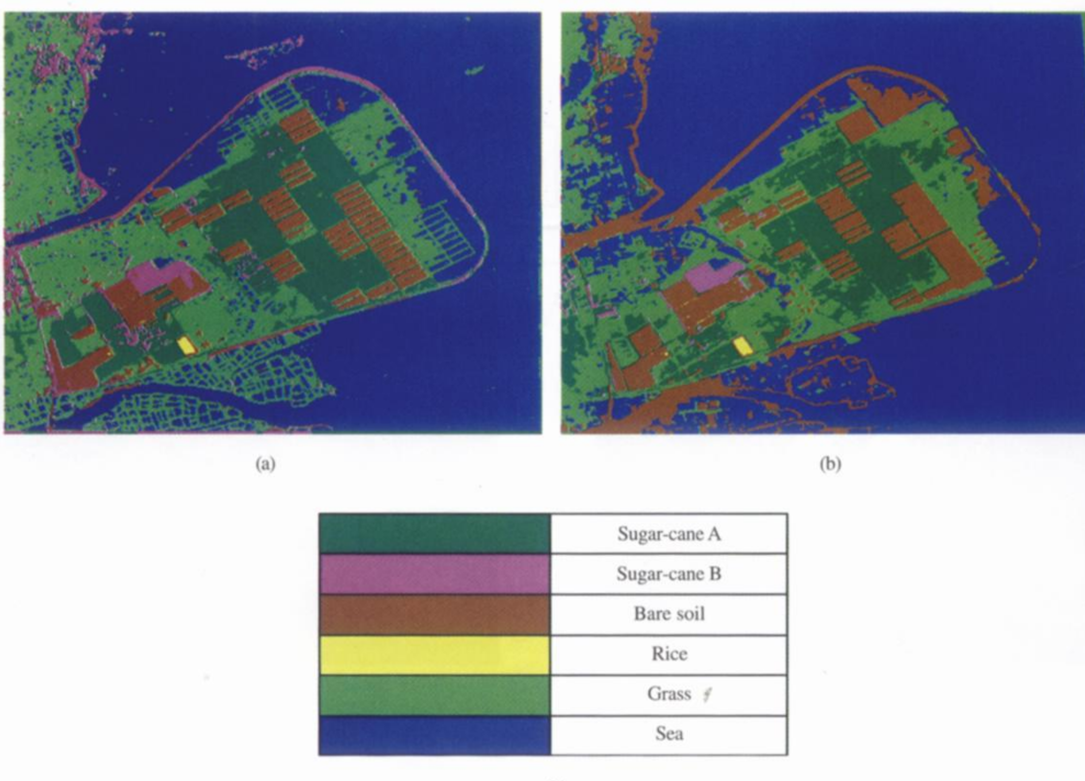

Fig. 6 (a) Classified result of fusion image; (b) Classified result of SPOT image; (c) Color table of each class

3.3 Classification Results of Feature-level Image Fusion

By following the working flow chart of feature-level image fusion (Fig 2), we classified those data sets by maximum likelihood classifier based on complex Wishart distribution for POLSAR data and multivariate Gaussian distribution for SPOT data. Fig 7 shows the classified results for both POLSAR and SPOT data. Fig 8 shows the fusion result. Table 3 shows the error matrix for POLSAR classified result and fusion result. Table 4 shows the error matrix for SPOT and fusion result. Table 5 shows fusion result for total seven classes. From the error matrix we can compute the overall accuracy and kappa coefficient, as shown in table 6.

Table 1　Error matrix for SPOT classified result

Classification	Ground truth						Total
	Sugarcane A	Sugarcane B	Grass	Rice	Bare soil	Sea	
Sugarcane A	3751	18	507	8	11	0	4295
Sugarcane B	0	727	3	0	3	0	733
Grass	971	0	987	8	24	7	1997
Rice	0	0	0	262	0	0	262
Bare soil	0	10	0	44	1279	583	1916
Sea	0	0	0	0	4	1300	1304
Total	4722	755	1497	322	1321	1890	10507

Table 2　Error matrix for fusion image classified result

Classification	Ground truth						Total
	Sugarcane A	Sugarcane B	Grass	Rice	Bare soil	Sea	
Sugarcane A	4628	7	12	0	14	0	4661
Sugarcane B	94	748	0	0	0	0	842
Grass	0	0	1485	0	0	41	1353
Rice	0	0	0	242	0	0	242
Bare soil	0	0	0	80	1298	5	1383
Sea	0	0	0	0	4	1844	1844
Total	4722	755	1497	322	1321	1890	10507

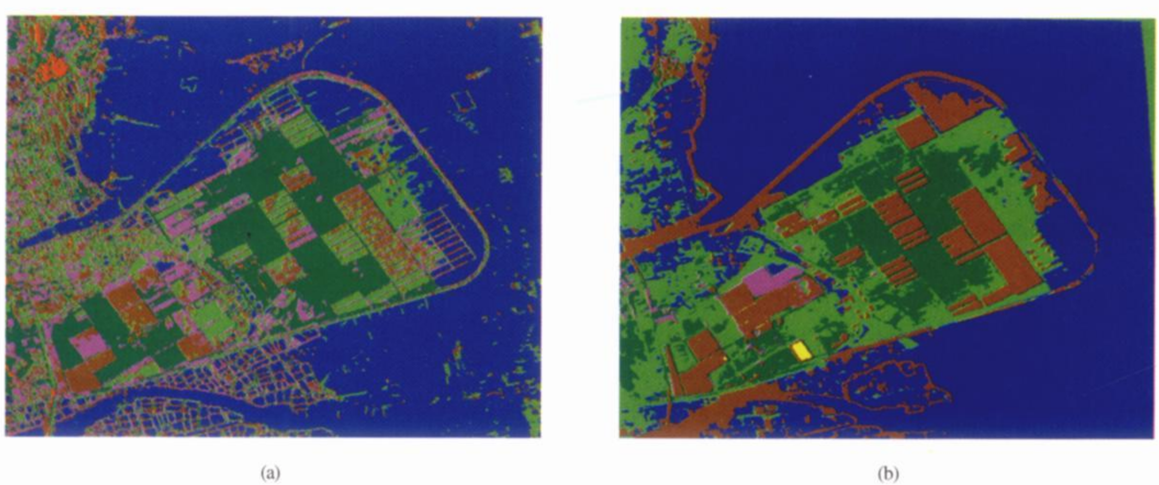

Fig.7　(a) POLSAR classified result; (b) SPOT classified result

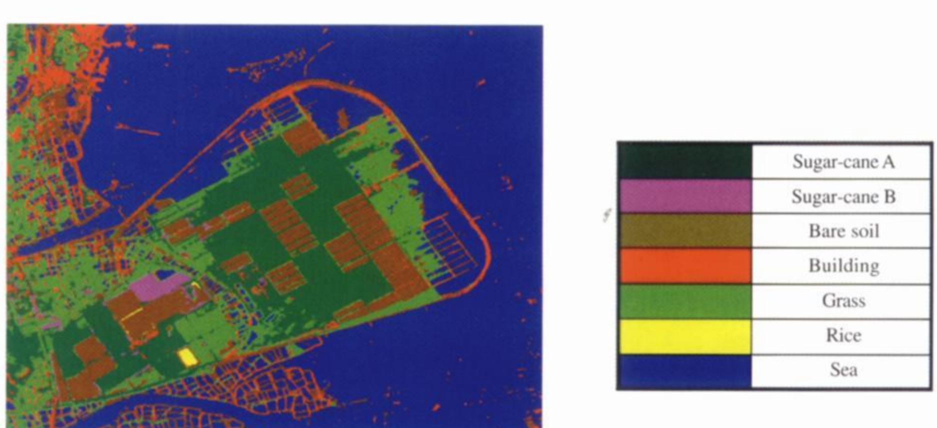

Fig.8　Fusion result

Table 3 (a) Error matrix for POLSAR classified result; (b) Error matrix for fusion result

(a)

Ground truth	Classification						Total
	Sugarcane A	Sugarcane B	Grass	Building	Bare soil	Sea	
Sugarcane A	4716	6	0	0	0	0	4722
Sugarcane B	155	290	30	0	280	0	755
Grass	55	424	1009	0	9	0	1497
Building	132	0	0	498	0	0	630
Bare soil	35	531	254	0	501	0	1321
Sea	0	1	2	0	2	1885	1890
Total	5093	1252	1295	498	792	1885	10815

(b)

Ground truth	Classification						Total
	Sugarcane A	Sugarcane B	Grass	Building	Bare soil	Sea	
Sugarcane A	4722	0	0	0	0	0	4722
Sugarcane B	10	728	4	0	13	0	755
Grass	272	2	1223	0	0	0	1497
Building	86	0	0	544	0	0	630
Bare soil	10	2	13	0	1296	0	1321
Sea	0	0	0	0	25	1865	1890
Total	5100	732	1240	544	1334	1865	10815

Table 4 (a) Error matrix for SPOT classified result; (b) Error matrix for fusion result

(a)

Ground truth	Classification						Total
	Sugarcane A	Sugarcane B	Grass	Rice	Bare soil	Sea	
Sugarcane A	3751	0	971	0	0	0	4722
Sugarcane B	18	727	0	0	10	0	755
Grass	507	3	987	0	0	0	1497
Rice	8	0	8	262	44	0	322
Bare soil	11	3	24	0	1279	4	1321
Sea	0	0	7	0	583	1300	1890
Total	4295	733	1997	262	1916	1304	10507

(b)

Ground truth	Classification						Total
	Sugarcane A	Sugarcane B	Grass	Rice	Bare soil	Sea	
Sugarcane A	4722	0	0	0	0	0	4722
Sugarcane B	10	728	4	0	13	0	755
Grass	272	2	1223	0	0	0	1497
Rice	0	0	18	254	50	0	322
Bare soil	10	2	13	0	1296	0	1321
Sea	0	0	0	0	25	1865	1890
Total	5014	732	1258	254	1384	1865	10507

Table 5　Error matrix for fusion result(seven classes)

Ground truth	Classified(result)							Total
	Sugarcane A	Sugarcane B	Grass	Rice	Bare soil	Sea	Building	
Sugarcane A	4722	0	0	0	0	0	0	4722
Sugarcane B	10	728	4	0	13	0	0	755
Grass	272	2	1223	0	0	0	0	1497
Rice	0	0	18	254	50	0	0	322
Bare soil	10	2	13	0	1296	0	0	1321
Sea	0	0	0	0	25	1865	0	1890
Building	86	0	0	0	0	0	544	630
Total	5100	732	1258	254	1384	1865	544	11137

Table 6　Overall accuracy and kappa coefficient for each of classified and fusion result

Result	Overall accuracy /%	Kappa coefficient /%
POLSAR classified result	82.28	75.65
Fusion result (Six classes, rice not included)	95.96	94.43
SPOT classified result	79.05	71.62
Fusion result (Six classes, building not included)	96.01	94.41
Fusion result (Seven classes)	95.47	93.86

4　CONCLUSION

In pixel-level fusion case, the classified result shows that grass and sugar-cane A could not be classified properly. When a single polarization (HV polarization, relatively sensitive to the vegetation canopy) added to the SPOT data by principle component analysis, it successfully solved the confusion problem in the original data. Overall accuracy and kappa coefficient shows the evidence. In feature-level fusion case, when we classify both data sets (POLSAR and SPOT data) individually, the classified results show the confusion problem for both of data sets, as the problem occured in pixel-level fusion case. When two data sets combined together by using Dempster-Shafer evidence theory, it also solved the confusion problem. Another advantage of feature-level image fusion is its ability to deal with ignorance and missing information. The last level, decision-level has not been implemented. It should take into account for future study.

References

[1]　Hall D L. Mathematical Techniques in Multisensor Data Fusion. Artech House, 1992.

[2]　Genderen J L Van, POHL C. Image Fusion: Issues, Techniques and Applications[A]. Intelligent Image Fusion, Proceedings EARSeL Workshop[C]. Strasbourg, France, 11 Sep. 1994.

[3]　Keys L D, Schmidt N J, Phillips B E. A Prototype Example of Sensor Fusion Used for a Siting Analysis[A]. Technical Papers, ACSM-ASPRS Annual Convention, Image Processing and Remote Sensing[C]. 1990, 4: 238—249.

[4]　Rogers R H, Wood L. The History and Status of Merging Multiple Sensor Data: an Overview[A]. Technical Papers 1990, ACSM-ASPRS Annual Convention, Image Processing and Remote Sensing[C]. 1990, 4: 352—360.

[5]　Lee J S. Intensity and Phase Statistics of Multilook Polarimetric and Interferometric Imagery[J]. *IEEE Trans. Geosci. Remote Sensing*, 1994, 32: 1017—1028.

[6]　Le Hégarat-Mascle S, Bloch I, Vidal-Madjar D. Application of Dempster-Shafer Evidence Theory to Unsupervised Classification in Multisource Remote Sensing[J]. *IEEE Trans. Geosci. Remote Sensing*, 1997, 35: 1018—1031.